www.czasopisma.pan.pl PAN POLSKA AKADEMIA NAUK www.journals.pan.pl

Arch. Metall. Mater. **67** (2022), 2, 677-684

DOI: https://doi.org/10.24425/amm.2022.137805

FAKHRYNA HANNANEE AHMAD ZAIDI[1], ROMISUHANI AHMAD[1,3], MOHD MUSTAFA AL BAKRI ABDULLAH[2,3*], WAN MASTURA WAN IBRAHIM[1,3], IKMAL HAKEM AZIZ[2,3], SUBAER JUNAIDI[4], SALMABANU LUHAR[5,3]

ASSESSMENT OF GEOPOLYMER CONCRETE FOR UNDERWATER CONCRETING PROPERTIES

For ages, concrete has been used to construct underwater structures. Concrete laying underwater is a very complex procedure important to the success or failure of underwater projects. This paper elucidates the influence of alkali activator ratios on geopolymers for underwater concreting; focusing on the geopolymer concrete synthesized from fly ash and kaolin activated using sodium hydroxide and sodium silicate solutions. The geopolymer mixtures were designed to incorporate multiple alkali activator ratios to evaluate their effects on the resulting geopolymers' properties. The fresh concrete was molded into 50 mm cubes in seawater using the tremie method and tested for its engineering properties at 7 and 28 days (curing). The control geopolymer and underwater geopolymers' mechanical properties, such as compressive strength, water absorption density, and setting time were also determined. The differences between the control geopolymer and underwater geopolymer were determined using phase analysis and functional group analysis. The results show that the geopolymer samples were optimally strengthened at a 2.5 alkali activator ratio, and the mechanical properties of the control geopolymer exceeded that of the underwater geopolymer. However, the underwater geopolymer was determined to be suitable for use as underwater concreting material as it retains 70% strength of the control geopolymer.

Keyword: Geopolymer; Underwater concrete; Fly ash; Kaolin

1. Introduction

Concrete has been used as a building material for underwater works for centuries. The underwater placement of concrete is a critically complex operation vital to underwater structures' success or failure [1]. The fresh concrete must not come into contact with the underwater fluids. Concrete can be placed underwater via excellent design and the appropriate method, which is vital as concrete placed underwater are vulnerable to cement washout, laitance, segregation, cold joints, and water entrapment [2]. Erosion caused by the marine environment can also destroy the concrete structure and compromise the quality of the products [3], which means that the underwater concrete needs to have excellent mechanical properties that would enable it to withstand its harsh environment. Mineral additives such as silica fume, fly ash and blast furnace slag are known to replace Portland cement to strengthen the concrete's structure [4]. However, the introduction of foreign elements into the concrete and its enhancement could come at the cost of other concrete properties.

Geopolymer material has been proposed as an alternative building material to Portland cement due to its high strength and resistance to chemical attacks [5-7]. Geopolymer is typically synthesized by mixing aluminosilicate-reactive material with a robust alkali solution such as sodium hydroxide (NaOH) and sodium silicate [8]. Due to its high silica and aluminium concentrations, fly ash is currently used to produce geopolymer materials [9,10]. There are 2 types of fly ash; classes C and F, classified by its total concentrations of Si, Fe, and Al [11]. The class C fly ash, also known as high calcium fly ash, is characteristically different from class F fly ash due to its higher Ca content inducing higher strength and lowering its setting time. The quick setting of fly ash class C makes it necessary to retard the setting time to allow for more efficient mixing, pouring, and geopolymerization. Yahya et al. stated that the addition of kaolin provides extra Si and Al for the geopolymerization reactions [12], which results in higher strength and prolonged setting times [13,14].

[1] UNIVERSITI MALAYSIA PERLIS, FACULTY OF ENGINEERING TECHNOLOGY, SUNGAI CHUCHUH, 02100 PADANG BESAR, PERLIS, MALAYSIA
[2] UNIVERSITI MALAYSIA PERLIS, FACULTY OF CHEMICAL ENGINEERING TECHNOLOGY, TAMAN MUHIBBAH, 02600 JEJAWI, ARAU, PERLIS, MALAYSIA
[3] UNIVERSITI MALAYSIA PERLIS (UNIMAP), PGEOPOLYMER & GREEN TECHNOLOGY, CENTRE OF EXCELLENCE (CEGEOGTECH), PERLIS, MALAYSIA
[4] UNIVERSITAS NEGERI MAKASSAR, GEOPOLYMER & GREEN MATERIAL GROUP, PHYSICS DEPARTMENT, FMIPA, INDONESIA
[5] FREDERICK RESEARCH CENTER, P.O BOX 24729, 1303 NICOSIA, CYPRUS

* Corresponding author: mustafa_albakri@unimap.edu.my

To decrease the rate of geopolymerization reactions, kaolin can be added to the fly ash at a concentration of 10%. However, it should be pointed out that exceeding this concentration increases the geopolymer's viscosity, which would render it unsuitable for underwater concreting methods as it requires good slump value.

Besides having a suitable aluminosilicate source material, the alkali activator solution plays a significant role in the dissolution of silica and alumina for geopolymerization [15]. This paper elucidates the influence of the alkali activator ratio on the mechanical properties of the underwater geopolymer. The effect of the underwater concreting method on geopolymer was also identified by comparing the compositions of the control geopolymer and underwater geopolymer.

2. Experimental Method

2.1. Materials

The raw fly ash was obtained from the Manjung Power Plant, Lumut, Perak, Malaysia. The low calcium variant (Class C) was used as the geopolymer's base material, as stipulated in the ASTM C618. The Associated Kaolin Industries Malaysia supplied the kaolin used in this study, which acted as the Si-Al source material. The chemical composition of the fly ash and kaolin are tabulated in TABLE 1. The sodium hydroxide (NaOH) powder was of caustic soda micro-pearls and 99% pure, brand name Formosoda-P. The sodium silicate (Na_2SiO_3) solution has a chemical composition of 30.1% SiO_2, 9.4% Na_2O and 60.5% H_2O, and was supplied by the South Pacific Chemicals Industries Sdn. Bhd., Malaysia.

TABLE 1

Chemical composition analysis of Fly ash class C and Kaolin powder

Element	SiO_2	Al_2O_3	CaO	Fe_2O_3	TiO_2	K_2O
Kaolin	54.0	31.7	—	4.89	1.41	6.05
Fly Ash	31.4	13.2	23.3	25.44	1.00	1.59

2.2. Sample Preparation

The geopolymer was prepared by dry mixing fly ash and kaolin, then adding the alkali activator solution to the mixture. The ratio of fly ash/ kaolin was kept constant at 10% based on previous research [12]. The alkali activator solution was prepared by dissolving sodium hydroxide pellets and mixing it with sodium silicate for at least 5 minutes until homogeneous. The freshly mixed geopolymer was poured into designated molds (per pouring method), then cured for 28 days before testing.

All of the geopolymer pastes were made with high calcium fly ash and kaolin powder. TABLE 2 shows the design proportions of the geopolymer mortar. The alkali activator ratio's effect was inspected by varying the ratios (2.0, 2.5, and 3.0), while the sodium hydroxide molarity and the solid-to-liquid ratio were kept constant at 12 M and 2.0, respectively. For each geopolymer design, 2 types of pouring method were used: the tremie method for the underwater geopolymer and the control method (cast in room temperature) for the control geopolymer. A tremie method is a pipe long enough to reach the concrete deposition site from above the water as shown in Figure 1.

TABLE 2

Mix design

Sample	NaOH molarity	Solid/liquid	Pouring method	Na_2SiO_3/ NaOH
1A	12M	2.0	Tremie	2.0
1B			Control	
2A			Tremie	2.5
2B			Control	
3A			Tremie	3.0
3B			Control	

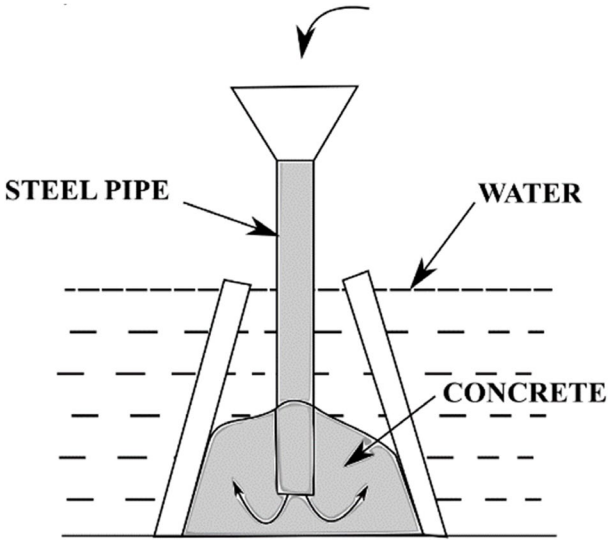

Fig. 1. Tremie Method

2.3. Testing and Characterization

2.3.1. Compressive Strength

Cubic molds were used to produce 50 mm samples for the compressive strength tests, according to the ASTM C109/ C109M – 16a using the Instron machine series 5569 Mechanical Tester after 7 and 28 days of exposure.

2.3.2. Density

Density is defined as the mass per unit volume. The density of the geopolymers was determined according to the ASTM C138 using the equation below. Three measurements were taken, and the average value was reported to ensure the repeatability of the

measurement. The mass and dimensions were also determined and reported.

$$\text{Density, } \rho = \frac{\text{Mass, } M}{\text{Volume, } V}$$

2.3.3. Water Absorption

The water absorption test was conducted to determine the moisture content of the geopolymer paste. According to instructions in ASTM C140, the sample was weighed before and after dried in an oven. The sample was then immersed in distilled water for another 24 hours before being weighed again. The water absorption was calculated using Equation 3.3.

$$\text{Water absorption} = \frac{W_S - W_d}{W_d} \times 100$$

Where:

W_S – saturated weight of samples (g),
W_d – oven-dry weight of samples (g).

2.3.4. Morphology

Microstructure analyses were performed using the JSM-6460LA Scanning Electron Microscope (JEOL) to image the control and underwater geopolymer's microstructures at different alkali activator ratios and curing days. The samples were prepared by coating it with Pt using the Auto Fine Coater JEOL JFC 1600. The chemical compositions of the geopolymer products were determined using the Energy X-ray Spectroscopy (EDX).

2.3.5. Setting Time

The duration of concrete hardening is one of the elements to prevent the segregation of concrete during underwater concreting. Thus, the setting time of the paste for each mix design is measured based on the penetration resistance using a Vicat needle according to ASTM C191.

2.3.6. Phase Analysis

The SHIMADZU diffractometer X-ray Diffraction (XRD) 6000 was used to identify the control geopolymer and underwater geopolymer samples' phases and crystallinities. The samples were prepared in powder form and pressed into aluminium holders. The operating conditions were 40 kV and 30 mA using Cu-Kα radiation. Data were collected using diffraction scans performed at 2θ of 10°-80° at a rate of 2°/min and a step size 0.02°. The X'Pert High Score Plus software was used to analyze the diffraction peaks.

2.3.7. Functional Group Analysis

The Perkin Elmer Spectrometer 2000 Fourier Transform Infrared (FTIR) spectroscopy is used to identify the chemical bonding of raw materials and fly ash/kaolin geopolymer. The scan range used was 450 cm^{-1} to 4000 cm^{-1} and resolution for all the infrared spectra was 4 cm^{-1}.

3. Results and discussion

3.1. Compressive Strength

Figure 2 shows the compressive strengths of the underwater geopolymer with various sodium silicate-to-sodium hydroxide ratios. When the ratio increases from 1.5 to 2.5, the compressive strength increases steadily from 17.64 MPa to its optimum value of 46.71 MPa, which can be attributed to the increasing silicate content reacting with the aluminosilicate source of the fly ash and kaolin to form sodium aluminosilicate networks, which harden and solidify the geopolymer [16]. Therefore, a higher silicate content resulted in higher strength observed in the alkali activator ratio's optimum value at 2.5. Increasing the ratio to 3.0 resulted in the compressive strength decreasing to 20.87 MPa due to excess silicate hindering water evaporation and structure formation during the geopolymerization process.

The underwater geopolymer's strength tends to increase with increasing curing times, from 7 days to 28 days, in all cases. Longer curing times increase the chances for the geopolymerization process to occur. The sample cured for 28 days is stronger relative to the samples cured for 7 days. The strength development of the underwater geopolymers at 1.5, 2.0, 2.5 and 3.0 alkali activator ratios resulted in increases of 21.1%, 48.2%, 45.4%, and 14.6%, respectively. Although the samples' strength increased in tandem with curing times, it can also be observed that when the alkali activator ratio exceeds 3.0, the geopolymer's strength only increases by 14.6% relative to the 45.4% increase when a 2.5 alkali activator ratio was used. Therefore, it can be concluded that a suitable alkali activator ratio results in higher strengths and induces a better strength development for the geopolymer.

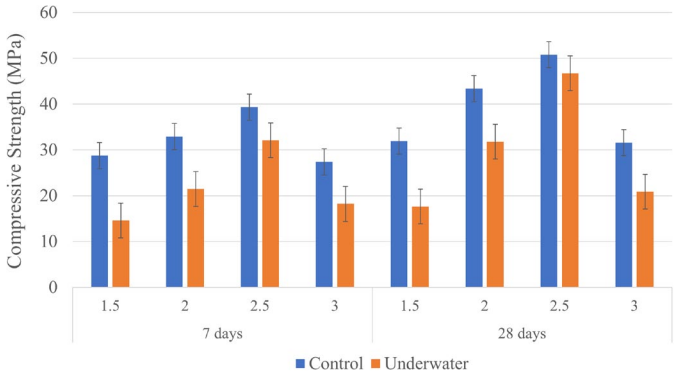

Fig. 2. Compressive strength of control geopolymer and underwater geopolymer with different alkali activator ratios at 7 and 28 days

The control geopolymer sample was observed to have a higher compressive strength relative to the underwater geopolymer sample for all alkali activator ratios and curing days variations. This can be attributed to the different pouring methods and the fact that the underwater geopolymer is susceptible to the surrounding seawater. For the underwater method, the fresh geopolymer was directly poured into a mold containing water. The fresh materials were likely to be subject to external forces in the surrounding water, causing the washout of unbonded materials during pouring. Grzecszczyk et al. pointed out that washout will not only decrease concrete strength; it also pollutes the surrounding water [2]. It can also be seen that the strength difference between the control geopolymer and underwater geopolymer is higher when using the 1.5 alkali activator ratio relative to that of 2.5. At an optimal ratio of 2.5, the underwater geopolymer retained 92% strength of the control geopolymer. In comparison, the underwater geopolymer at a 1.5 alkali activator ratio can only retain 55% of the control geopolymer's strength, proving that there is less material damaged from the washout process when an optimum mix design is used.

3.2. Density

The density of the underwater geopolymer with different alkaline activator ratios is shown in Figure 3. It can be seen that the density of fly ash/kaolin geopolymer increases as the alkaline activator increases, up to 2.5, then decreases at ratio 3.0, similar to the trend displayed by the compressive strength. A higher density represents a well-developed geopolymerization process with denser matrices and low porosities. Ramasamy et al. posited that the increase in density could be attributed to the excellent sodium silicate content, which prompted the geopolymerization process towards producing a denser matrix [17]. The highest density (2116.08 kg/m^3) is recorded when using a 2.5 ratio of alkaline activator, while the lowest density (1821 kg/m^3) is realized using a 1.5 ratio of alkaline activator. The decrease in density at 3.0 was caused by the inability to form a complete geopolymer network.

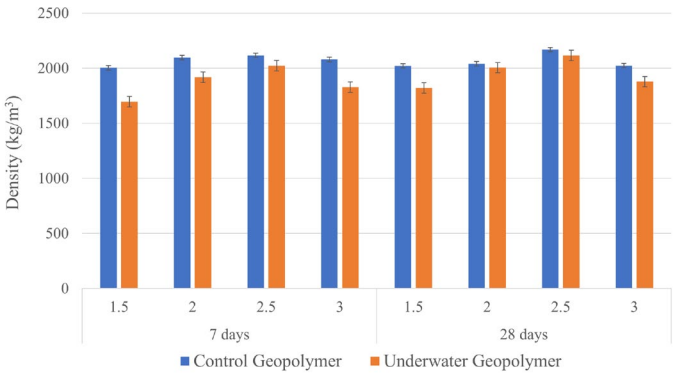

Fig. 3. The density of control geopolymer and underwater geopolymer with different alkali activator ratio at 7 and 28 days

3.3. Water Absorption

The water absorption of the underwater geopolymers with different alkaline activator ratio is presented in Figure 4. It can be seen that as the alkaline activator ratio increases up to 2.5, the water absorption percentage decreases. The lowest water absorption of 0.12% is evident when using a 2.5 alkaline activator ratio, while the highest water absorption of 0.41% is achieved when using a 1.5 alkaline activator ratio. Lower water absorption is preferred due to its lower porosity. This trend agrees with the trend exhibited by the density of fly ash/kaolin geopolymer for underwater concreting, where the sample using 2.5 ratios resulted in the highest density. According to Ibrahim et al., at lower alkaline activator ratios, the workability of the mixture is low, which results in poor bonding between the raw materials and alkaline activators, which increases the possibility of segregation and cement washout during concrete placement [18], resulting in low strength, density, and water absorption.

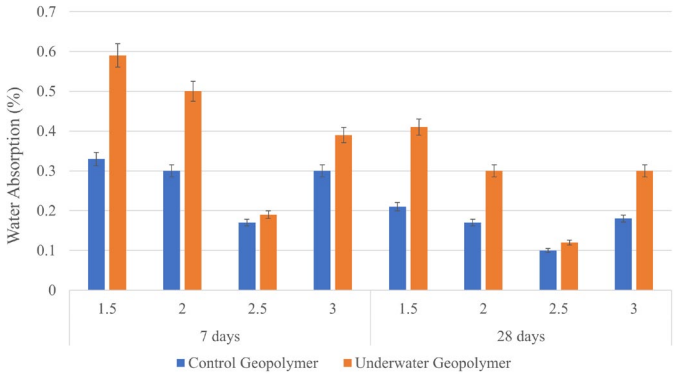

Fig. 4. Water absorption of control geopolymer and underwater geopolymer with different alkali activator ratio at 7 and 28 days

3.4. Morphology

The microstructure images of the underwater geopolymers at 1.5, 2.0, 2.5 and 3.0 alkali activator ratios for control geopolymer and underwater geopolymer are shown in Figure 5. The SEM micrograph shows a change in the structure of the underwater geopolymer with increasing alkali activator ratios. It can be seen that the sample at 1.5 and 2.0 alkaline activator ratios contain an abundance of pores and unreacted fly ash. As the alkali activator ratio increased to 2.5, the samples' microstructure seems to be relatively well-developed with lower porosities and unreacted fly ash. Higher alkali activator ratio is equivalent to higher silicate content, which is required for the geopolymerization process. The results agree with those of the compressive strength, density and water absorption discussed previously, where the optimal geopolymer properties are obtained when using an alkali activator ratio of 2.5.

Similarly, the differences between control geopolymer and underwater geopolymer were also in agreement with the compressive strength results. The control geopolymer has a better microstructure, with lower porosities and unreacted fly ash

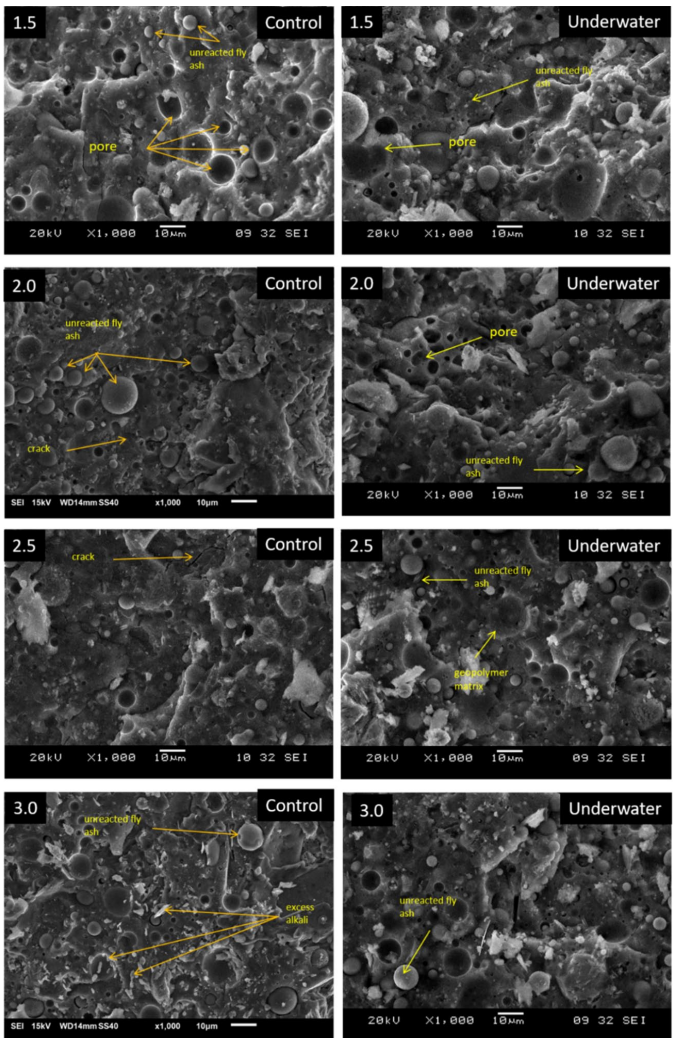

Fig. 5. Morphology of control geopolymer and underwater geopolymer with different alkali activator ratio

relative to the underwater geopolymer. Further increasing the alkali activator ratio to 3.0 resulted in flake-like white particles known as efflorescence. Phoo-ngernkham et al. [19] reported that additional silicate produces enough geopolymer gels to fill the space between the particles, resulting in higher density geopolymer matrices . Nonetheless, when the alkali activator exceeds its optimum value, efflorescence is formed, indicating excess alkali content. Phoo-ngernkham et al. (2015) sited that efflorescence distorts the geopolymerization, which resulted in a compromised mechanical property [20].

3.5. Setting Time

The setting time of geopolymer with different alkaline activator ratio is shown in Figure 6. The final setting time ranged from 30 min to 45 min. It was observed that the longest setting time of 45 min is obtained by using 1.5 alkaline activator ratio. The setting time then steadily decrease as the alkaline activator ratio increase where the shortest setting time (30 min) is noted by using alkaline activator ratio of 3.0. This result corresponds to the formation of aluminosilicate gel during the geopolymerization process. As the alkaline activator ratio increases, the silicate content supply for geopolymerization process increased thus accelerates the dissolution process of Si and Al causing the geopolymer to set faster.

However, short setting time also causes the inability of normal geopolymerization to occur since the mixture hardens before the reaction was completed. This corresponds to the compressive strength result of sample where geopolymer using 3.0 alkali activator ratio with low setting time presents lower compressive strength compared to 2.5 alkali activator ratio. According to Ibrahim et al., in terms of underwater concreting material, lower setting time are preferred to reduce the washout and segregation due to contact with surrounding water . Thus, 2.5 alkali activator ratio was chosen as the optimum ratio since it provides low setting time without relinquish the strength, density and water absorption [18].

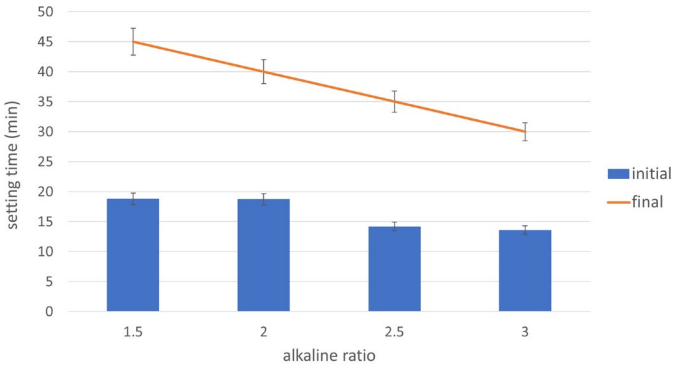

Fig. 6. Setting time of fly ash/kaolin geopolymer with different alkaline activator ratio

3.6. Phase Analysis

Figure 7 shows the XRD diffractogram of the control geopolymer and underwater geopolymer. The phase characterization was conducted to elucidate the curing method's influence on the control geopolymer and underwater geopolymer based on the optimum mix design, which is 2.5. The phases of the underwater geopolymer are similar to that of the control geopolymer's. The peaks observed in the raw fly ash were identified as quartz, hematite, antigorite, and periclase, while raw kaolin has multiple peaks identified as quartz and kaolinite. The identifiable peaks present in the control geopolymer and underwater geopolymer were quartz, periclase, and calcite. The hematite and antigorite had peaks at 2θ of 33.4 and 35.6, respectively, although at lowered intensities in both geopolymer sample relative to that of the raw fly ash. The activation of fly ash with alkali solution leads to aluminosilicate gel formation with some crystalline phases, represented by the broad diffraction band at 20°-40°. It is speculated that the Ca, Si, Al was released during the geopolymerization process.

The phase analysis of the underwater geopolymer resulted in similar peaks to that observed in the control geopolymer.

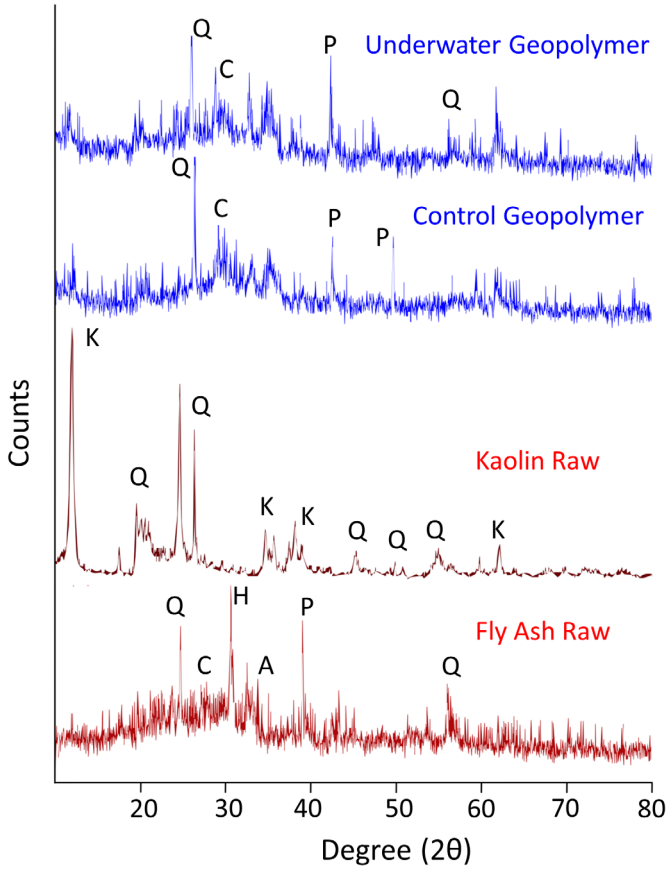

Fig. 7. XRD analysis of fly ash/kaolin geopolymer (control), underwater fly ash/kaolin geopolymer, raw kaolin and raw fly ash. (Q – quartz, P – periclase, C – calcite, H – Hematite, A – antigorite, K – kaolinite)

However, the latter has higher intensity peaks compared to the former. The calcite ($CaCO_3$) detected in the control geopolymer can be attributed to the Ca^{2+} dissolved from the fly ash reacting with OH^- in an alkali solution to form $Ca(OH)_2$ reacting with atmospheric CO_2, forming calcite during the geopolymerization, as per the equations below. It can be seen that the intensity of calcite in the control geopolymer exceeds that of the underwater geopolymer. The presence of calcite leads to the strength reinforcement of geopolymer, which explains the higher strength exuded by the fly ash/kaolin geopolymer relative to the underwater fly ash/kaolin geopolymer [21].

$$Ca^{2+}(aq) + OH^-(aq) \rightarrow Ca(OH)_2(s)$$

$$Ca(OH)_2(s) + CO_2(g) \rightarrow CaCO_3(s) + H_2O$$

In the underwater geopolymer case, the calcite peak was of lower intensity due to its seawater reaction. Seawater is generally supersaturated with calcite, but will not precipitate from natural seawater. However, Subhas et al., [22] believe that the addition of Ca^{2+} ions will induce precipitation. In this case, the Ca^{2+} ions supplied by the fly ash/kaolin geopolymer will precipitate calcite, which decreases the intensity of calcite peaks in the underwater fly ash/kaolin geopolymers. The schematic of the reaction occurred in underwater geopolymer sample is illustrated in Figure 8. The precipitation was analysed using SEM, and the results are shown in Figure 5 and TABLE 3, confirming that the precipitation consists of the mixture of calcite ($CaCO_3$) and salt (NaCl).

TABLE 3

Chemical composition of the precipitate

Element	Na	Mg	Si	Cl	Ca	C	O
At%	6.95	0.72	1.41	4.1	1.74	62.71	22.36

3.7. Functional Group Analysis

The IR spectra of underwater geopolymer and control geopolymer in the range of 400 cm^{-1} to 4000 cm^{-1} are shown

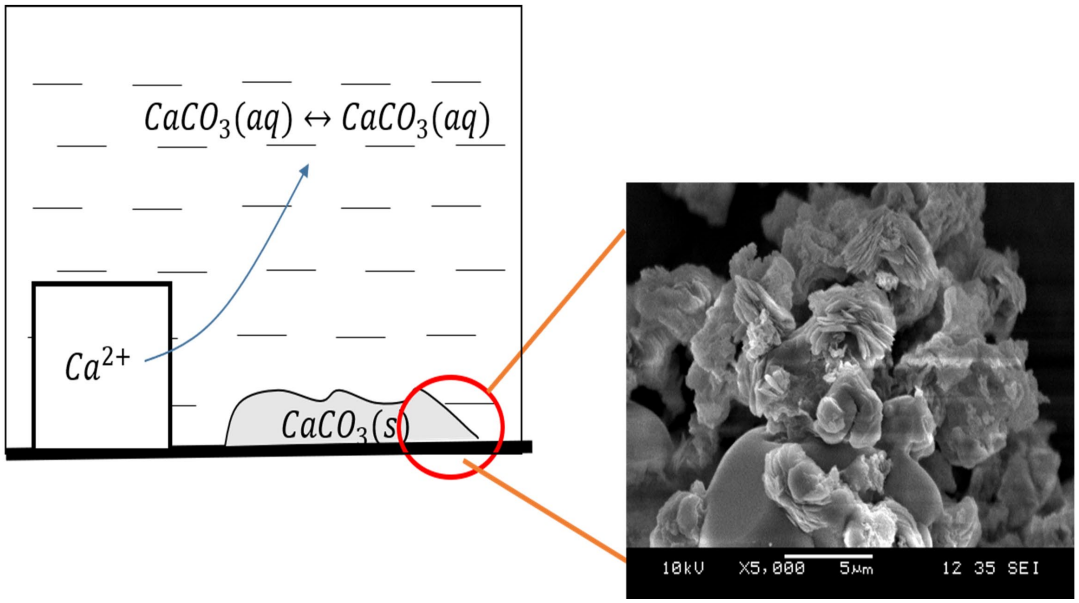

Fig. 8. Microstructure image of the precipitate

in Figure 9. Based on the IR spectrum given, both geopolymer sample shows a similar trend without any obvious changes. The IR spectrum of control geopolymer and underwater geopolymer at 2θ = 3445.06 cm^{-1} to 1652.28 cm^{-1} and 3450.58 cm^{-1} to 1646.85 cm^{-1} respectively indicates the stretching and deformation of OH and H-O-H groups from the weakly bound water molecules absorbed or trapped in the large cavities between the rings of geopolymeric product. The peak approximately at 1433.70 cm^{-1} and 1465.97 cm^{-1} for control geopolymer and underwater geopolymer indicates the stretching vibration of O-C-O. The asymmetric stretching of Si-O-Si and Al-O-Si can be characterized at bands 1012.22 cm^{-1} for control geopolymer and 1017.56 cm^{-1} for underwater geopolymer. The bands 689.66 cm^{-1} and 695.92 cm^{-1} characterize the asymmetric vibration of Si-O-Si in quartz. While the bending vibration of Si-O-Al is shown at bands 542.07 cm^{-1} and 541.09 cm^{-1}. Finally, the bending vibration of H-O-H can be seen at band 467.05 cm^{-1} and 466.48 cm^{-1}.

Although the control geopolymer and underwater geopolymer showed similar IR spectrum wavelength, it can be observed that control geopolymer presents lower transmittance (%T) when compared to underwater geopolymer. This lower transmittance indicates higher stability and more condensed aluminosilicates matrix. Thus, explains the higher strength of control geopolymer compared to underwater geopolymer according to the previous compressive strength result. Research by Liew et al. [23] and Allah et al. [24] also agrees on this strength relation.

4. Conclusion

This paper detailed an experimental investigation into the production of underwater geopolymer from fly ash and kaolin with sodium silicate and sodium hydroxide as its alkali activator. The geopolymer was made up of 12M sodium hydroxide, 2.0 solid-to-liquid ratio, and 2.5 sodium silicate-to-sodium hydroxide ratio, was poured into a mold underwater using the tremie method to produce a material that has a compressive strength of 46.71 MPa, a density of 2.12 kg/m^3, and water absorption of 0.12%. This product was then compared to the control geopolymer sample to elucidate the different pouring method's influence on the geopolymers, and the underwater polymer exhibited compromised strengths. The underwater geopolymer's lowered strength was also confirmed via phase analyses, where the lowered calcite phase in the underwater geopolymer indicates that the Ca (strength element in the product) in the geopolymer were dissolved in the seawater and precipitated. However, despite the slightly compromised strength of the underwater geopolymer,

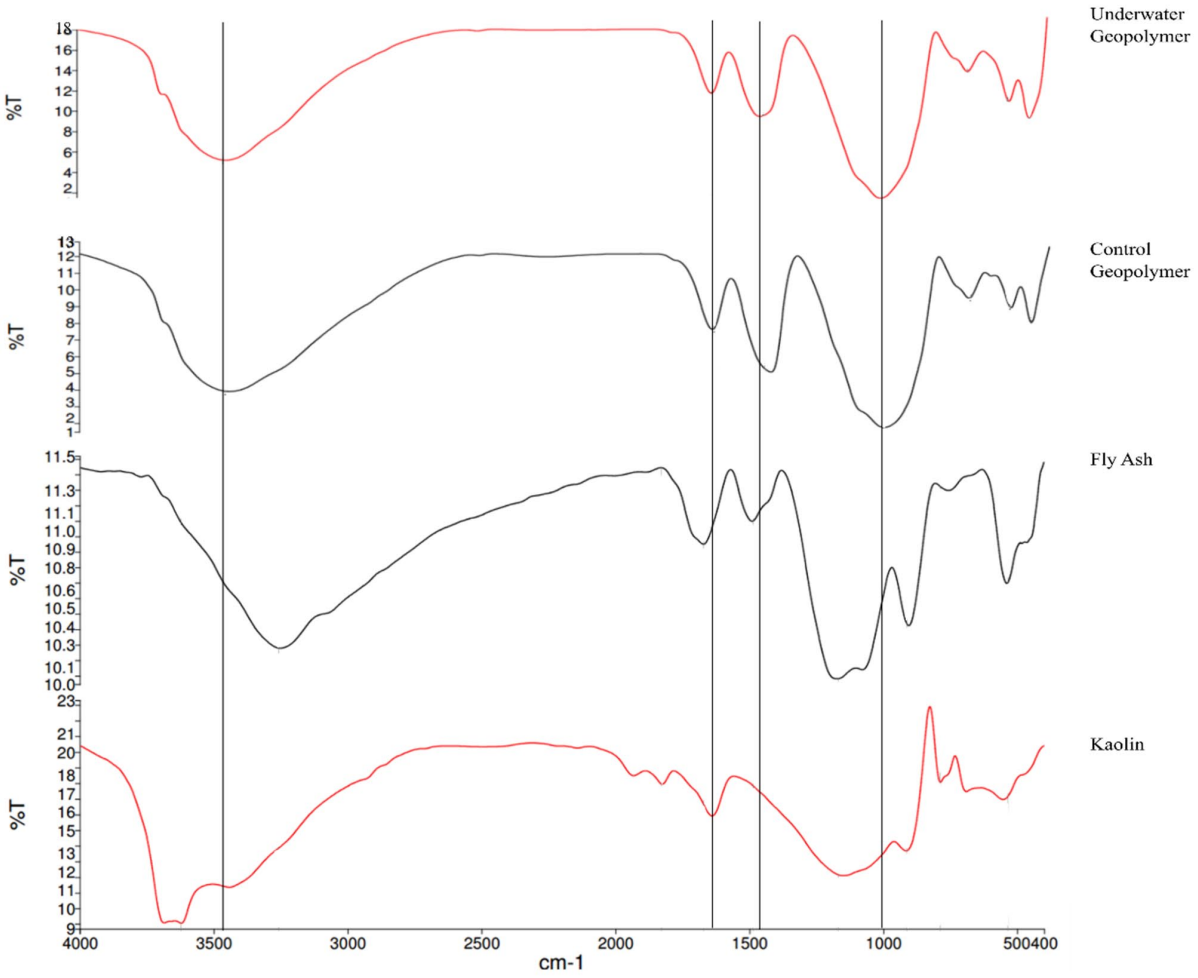

Fig. 9. FTIR spectra of, control geopolymer and underwater geopolymer, raw kaolin, and raw fly ash

it retains 92% strength relative to the control geopolymer, and as per the JSCE guidelines, makes it suitable for use as underwater concreting material.

Acknowledgement

The authors wish to acknowledge the Center of Geopolymer and Green Technology for providing the laboratory facilities. This work was funding supported by the "Partnership for Research in Geopolymer Concrete" (PRIGeoC-689857) sponsored by the European Union.

REFERENCES

[1] F. Pacheco-Torgal, J. Labrincha, C. Leonelli, A. Palomo, P. Chindaprasit, Handbook of alkali-activated cements, mortars and concretes, Elsevier (2014).

[2] S. Grzeszczyk, K. Jurowski, K. Bosowska, M. Grzymek, Constr. Build. Mater. **203**, 670-678 (2019).

[3] J. Hwalla, M. Saba, J.J. Assaad, Mater. Struct. **53**, 1-14 (2020).

[4] W. Lv, Z. Sun, Z. Su, Cem. Concr. Compos. **106**, 103484 (2020).

[5] R. Ahmad, M.M.A.B. Abdullah, W.M.W. Ibrahim, K. Hussin, F.H. Ahmad Zaidi, J. Chaiprapa, J.J. Wysłocki, K. Błoch, M. Nabiałek, Materials **14**, 1077 (2021).

[6] E.A. Azimi, M.M.A. Al Bakri, Y.M. Liew, C.Y. Heah, K. Hussin, I.H. Aziz, Review of geopolymer materials for thermal insulating applications, in: Key Engineering Materials (2015).

[7] A.M. Aguirre-Guerrero, R.A. Robayo-Salazar, R.M. de Gutiérrez, Appl. Clay Sci. **135**, 437-446 (2017).

[8] R. Ahmad, M. Abdullah, K. Hussin, A.V. Sandu, M. Binhussain, N.A. Jaya, Rev. Adv. Mater. Sci. **44**, 26-32 (2016).

[9] H. Fansuri, W.S. Subaerb, D. Hartantoa, N. Widiastutia, Chem. Eng. **72**, (2019).

[10] A. Karthik, K. Sudalaimani, C.V. Kumar, Constr. Build. Mater. **149**, 338-349 (2017).

[11] A. Falmata, A. Sulaiman, R. Mohamed, A. Shettima, SN Appl. Sci. **2**, 1-11 (2020).

[12] Z. Yahya, M. Abdullah, N.M. Ramli, D. Burduhos-Nergis, R. Abd Razak, Influence of Kaolin in fly ash based geopolymer concrete: destructive and non-destructive testing, in: IOP Conference Series: Materials Science and Engineering (2018).

[13] G.F. Huseien, J. Mirza, M. Ismail, S. Ghoshal, M.A.M. Ariffin, Ain Shams Eng. J. **9**, 1557-1566 (2018).

[14] I.H. Aziz, M.M.A. Al Bakri, C.Y. Heah, L. Yun Ming, K. Hussin, E.A. Azimi, A review on mechanical properties of geopolymer composites for high temperature application, in: Key Engineering Materials (2015).

[15] C.-L. Hwang, T.-P. Huynh, Constr Build Mater. **101**, 1-9 (2015).

[16] H.Y. Leong, D.E.L. Ong, J.G. Sanjayan, A. Nazari, Constr. Build. Mater. **106**, 500-511 (2016).

[17] Z. Dong, A. Bouaissi, X. Wang, Y. Huang, L.-Y. Li, M.M.A.B. Abdullah, S. Ramasamy, Adv. Eng. Mater. **21**, 1900621 (2019).

[18] O.M.O. Ibrahim, A.M. Heniegal, K.G. Ibrahim, I.S. Agwa, Adv. Concr. Constr. **10**, 455-462 (2020).

[19] T. Phoo-Ngernkham, A. Maegawa, N. Mishima, S. Hatanaka, P. Chindaprasirt, Constr. Build. Mater. **91**, 1-8 (2015).

[20] Z. Zhang, H. Zhu, C. Zhou, H. Wang, Appl. Clay Sci. **119**, 31-41 (2016).

[21] M. Merabtene, L. Kacimi, P. Clastres, Heliyon. **5**, e01938 (2019).

[22] A.V. Subhas, J.F. Adkins, N. E. Rollins, J. Naviaux, J. Erez, W.M. Berelson, PNAS. **114**, 8175-8180 (2017).

[23] Y.-M. Liew, C.-Y. Heah, H. Kamarudin, Prog. Mater. Sci. **83**, 595-629 (2016).

[24] R. Abd Allah, A.S. Faried, W.H. Soufi, M.A. Abd El-Aziz, Am. J. Constr. Build. Mater. **2**, 78-85 (2017).